

# Brillouin Microscopy of Collagen Crosslinking: Noncontact Depth-Dependent Analysis of Corneal Elastic Modulus

Giuliano Scarcelli,<sup>1,2</sup> Sabine Kling,<sup>3</sup> Elena Quijano,<sup>1</sup> Roberto Pineda,<sup>4</sup> Susana Marcos,<sup>3</sup> and Seok Hyun Yun<sup>1,2,5</sup>

**PURPOSE.** Corneal collagen crosslinking (CXL) is designed to halt the progression of keratoconus and corneal ectasia by inducing corneal stiffening. However, it currently is difficult to monitor and evaluate CXL outcome objectively due to the lack of suitable methods to characterize corneal mechanical properties. We validated noncontact Brillouin microscopy to quantify corneal mechanical properties before and after CXL.

**METHODS.** CXL was performed on fresh porcine eyes using various presoaking times and light doses, with or without epithelial debridement. From Brillouin maps of corneal elastic modulus, stiffness and average modulus of anterior, middle, and posterior stroma were analyzed. Corneal stiffening index (CSI) was introduced as a metric to compare the mechanical efficacy of a given CXL protocol with respect to the standard protocol (30-minute riboflavin presoak, 3 mW/cm<sup>2</sup> ultraviolet illumination for 30 minutes).

**RESULTS.** Brillouin corneal stiffness increased significantly ( $P < 0.001$ ) by epi-off and epi-on CXL. The increase of Brillouin modulus was depth-dependent, indicating that anterior stromal stiffening contributes the most to mechanical outcome. The increase of anterior Brillouin modulus was linearly proportional to the light dose ( $R^2 > 0.98$ ). Compared to the standard epi-off procedure, a typical epi-on procedure resulted in a third of stiffness increase in porcine corneas (CSI = 33).

**CONCLUSIONS.** Brillouin microscopy allowed imaging and quantifying CXL-induced mechanical changes without contact in a depth-dependent manner at high spatial resolution. This technique may be useful to evaluate the mechanical outcomes of CXL procedures, to compare different crosslinking agents,

and for real-time monitoring of CXL in clinical and experimental settings. (*Invest Ophthalmol Vis Sci.* 2013;54:1418-1425) DOI:10.1167/iovs.12-11387

The decrease of corneal mechanical stability has a critical role in the onset and progression of keratoconus and post-LASIK ectasia.<sup>1</sup> Corneal collagen crosslinking (CXL) is a promising treatment that aims at stopping the progression of ectasia by increasing corneal stiffness.<sup>2</sup> CXL induces the formation of covalent bonds between collagen fibers in the corneal stroma by photoactivation of a photosensitizer, such as riboflavin. The increased number of the crosslinks increases the elastic modulus of the corneal tissue. CXL has been approved in Europe and is under clinical trials in the United States. The majority of CXL procedures follow the original "Dresden" protocol described by Wollensak et al.<sup>3</sup> Over the past decade, studies following the long-term clinical outcome of the treatment have shown that the CXL procedure effectively stops progression of ectasia in the majority of patients.<sup>4-6</sup> Recently, however, a great deal of interest has been placed towards devising new CXL protocols to minimize the damage to keratocytes and to reduce the recovery time post intervention.<sup>7-10</sup> In this respect, a central role is played by the epithelium: because the epithelium represents a major barrier for the diffusion of photosensitizers into the stroma, the standard Dresden protocol involves the removal of the epithelium, which results in delayed recovery and increased risks of infections; novel CXL procedures try to solve this issue by chemically loosening epithelial junctions,<sup>7,10</sup> or by custom epithelial debridement.<sup>9</sup>

Despite the advance in CXL, it has been difficult to measure, monitor, and optimize the defining feature that drives the clinical outcome of the different CXL protocols, that is corneal mechanical stiffening, due to the lack of noninvasive mechanical characterization tools able to assess the performance of different protocols in vivo.

Mechanical measurements traditionally are macroscopic and destructive.<sup>11</sup> Recently, a widespread effort to achieve a noninvasive test of corneal mechanical properties has been put forward. An ocular response analyzer measures corneal hysteresis.<sup>12</sup> Corneal hysteresis has been shown to correlate with CXL and advanced keratoconus,<sup>13,14</sup> but its clinical usefulness remains questionable.<sup>15,16</sup> Anterior segment imaging combined with an air puff has allowed dynamic measurements of corneal deformation, showing different deformation parameters in untreated corneas and crosslinked corneas.<sup>17</sup> This technique allows for in vivo measurements, but it remains challenging to determine the corneal biomechanical properties from the deformation images due to the contributions of the corneal geometry and intraocular pressure among other factors.<sup>17</sup> (Roberts CJ, et al. *IOVS* 2011;52:ARVO E-Abstract 4384). Other techniques based on

From the <sup>1</sup>Wellman Center for Photomedicine, Massachusetts General Hospital, Cambridge, Massachusetts; the <sup>2</sup>Department of Dermatology, Harvard Medical School, Boston, Massachusetts; the <sup>3</sup>Instituto de Optica, Consejo Superior de Investigaciones Cientificas (CSIC), Madrid, Spain; the <sup>4</sup>Department of Ophthalmology, Massachusetts Eye and Ear Infirmary, Boston, Massachusetts; and <sup>5</sup>Harvard-MIT Health Sciences and Technology, Cambridge, Massachusetts.

Supported by the Harvard Clinical and Translational Science Center (NIH UL1-RR025758), American Society for Laser Medicine and Surgery, National Institutes of Health (P41-EB015903), National Science of Foundation (CBET-0853773), Spanish Government (FIS2008-02065, FIS2011-25637), and the European Research Council (ERC-AdG-294099).

Submitted for publication November 27, 2012; revised January 3, 2013; accepted January 21, 2013.

Disclosure: G. Scarcelli, P; S. Kling, None; E. Quijano, None; R. Pineda, None; S. Marcos, None; S.H. Yun, P

Corresponding author: Seok Hyun Yun, 65 Landsdowne Street, UP-5, Cambridge, MA 02139; syun@hms.harvard.edu.

ultrasound<sup>18,19</sup> are under development.<sup>20–22</sup> Currently, to our knowledge no clinical device is capable of measuring directly the mechanical properties, such as the elastic modulus, of corneal tissue.

Recently, the feasibility of Brillouin microscopy<sup>23</sup> for mapping corneal modulus in three dimensions with a high spatial resolution has been demonstrated.<sup>24,25</sup> This optical technique is noninvasive, and does not involve structural or mechanical deformation of the cornea. In our study, Brillouin microscopy was applied to investigate the biomechanical properties of the cornea after various riboflavin-mediated CXL procedures. We evaluated the differential effect of light dose, photosensitizer soaking, hydration, and epithelial debridement on the mechanical outcome of CXL protocols. A corneal stiffening index (CSI) is introduced as a quantitative metric to compare the mechanical outcome of a CXL protocol to that of the standard Dresden protocol. The results provided novel insights on the mechanical effects of CXL procedures and demonstrated Brillouin microscopy as a valuable tool for assessing CXL mechanical performance.

## MATERIALS AND METHODS

### Brillouin Microscope

The Brillouin microscope platform is similar to the one described previously.<sup>24</sup> Briefly, it consisted of a confocal microscope with numerical aperture (NA) of 0.3 and a high-resolution optical spectrometer. A single-mode laser at a wavelength of 532 nm (Torus; Laser Quantum, Inc., San Jose, CA) illuminated the sample with a typical power of 7 mW. The lateral and axial resolutions were approximately 1 and 8  $\mu\text{m}$ , respectively. A custom-made chamber held the corneas flattened gently onto a plastic dish so that the laser light accessed the sample in an inverted configuration through the flattened surface. The holding chamber mounted on a motorized stage (Prior Scientific, Inc., Rockland, MA) enabled 3D translation of the sample. The scattered light from the sample was collected by a single-mode optical fiber (Thorlabs, Newton, NJ) and coupled into a two-stage VIPA spectrometer in the cross-axis configuration with sub-GHz frequency resolution.<sup>26,27</sup> The dispersed optical spectrum was recorded with an EM-CCD camera (Ixon Du197; Andor, Belfast, UK) with a frame integration time of 200 ms. The CCD data were processed to determine the Brillouin frequency shifts by using a custom-written MATLAB program. Brillouin images were produced by plotting the measured frequency shifts over space with color encoding.

### Brillouin Elastic Modulus

Brillouin light scattering arises from the interaction between photons and acoustic phonons (propagation of thermodynamic fluctuations) in a sample. The resulting frequency shift  $\Omega$  and the line width  $\Delta\Omega$  of the Brillouin spectrum are related to the longitudinal viscoelastic modulus  $M^*$ , which is composed of elastic modulus,  $M'$ , and viscous modulus,  $M''$ <sup>28</sup>:

$$M' = \frac{\rho\lambda^2\Omega^2}{4n^2} \quad \text{and} \quad M'' = \frac{\rho\lambda^2\Omega\Delta\Omega^2}{4n^2} \quad (1)$$

where  $\rho$  is the mass density,  $\lambda$  is the optical wavelength and  $n$  is the refractive index. To convert the Brillouin shift to the longitudinal modulus, the value of  $\rho/n^2$  is required. From literature values of the refractive index and density, which are spatially varying,<sup>29,30</sup> the ratio of  $\rho/n^2$  is approximately constant with a value of 0.57  $\text{g}/\text{cm}^3$  and a variation of less than 0.3% throughout the cornea.<sup>19,31</sup>

### Corneal Stiffening Index

The longitudinal modulus  $M'$  of a material can be expressed in terms of its standard Young's modulus  $E'$  via the Poisson's ratio  $\sigma$ , that is,  $M' = E'(1 - \sigma)/(1 + \sigma)(1 - 2\sigma)$ . In Brillouin measurements, the modulus  $M'$  is probed in a hypersonic frequency range of 5 to 10 GHz. It has been shown empirically that the Brillouin-measured longitudinal modulus  $M'$  is related to the conventional Young's (or shear) moduli  $E'$  through a log-log linear relationship:  $\log(M') = a \log(E') + b$ , where  $a$  and  $b$  are material-dependent coefficients.<sup>32</sup> From the log-log relationship, the change of elastic modulus induced by a CXL protocol can be written as:  $\Delta M'/M' = a \Delta E'/E'$ . From this relationship, it follows that the relative change of Brillouin modulus of two different procedures,  $\Delta M_2/\Delta M_1$ , is equal to the relative change of Young's modulus,  $\Delta E_2/\Delta E_1$ ; that is,

$$\frac{\Delta M_2'}{\Delta M_1'} = \frac{\Delta E_2'}{\Delta E_1'} \quad (2)$$

The CSI is defined as a quantitative measure of the mechanical outcome of a specific CXL procedure (denoted by a subscript X) in direct comparison to the traditional Dresden protocol:

$$CSI_X \equiv \frac{\Delta M_X'}{\Delta M'_{\text{Dresden}}} = 100 * \frac{\Delta E_X'}{\Delta E'_{\text{Dresden}}} \quad (3)$$

The CSI, therefore, compares the increase in corneal stiffness with respect to the standard CXL method. By definition, the CSI of the Dresden protocol is 100. Any procedures that resulted in a smaller modulus change would have CSI less than 100. For example, CSI is 50 for a procedure that increases elastic modulus half as much as the Dresden method. Interestingly, CSI allows universal comparison between mechanical tests that use very different methods to assess mechanical properties, for example Brillouin microscopy, stress-strain tests, and shear rheometry.

### Brillouin Measurement Protocols

All animals in this study were used in accordance with the ARVO Statement for the Use of Animals for Ophthalmic and Vision Research. Porcine eyes were obtained 2 to 4 hours postmortem (Research 87, Inc., Boylston, MA), and kept on ice during transport and storage until the starting of the experiments. The whole eye was placed in a chamber holder and flattened gently over a plastic dish to facilitate optical illumination/detection. Flattening the cornea did not alter its mechanical properties, as confirmed by control experiments of unflattened eyes resting suspended in a bath of saline solution or mineral oil. All reported experiments were conducted within 2 hours from tissue arrival. Brillouin measurements were obtained immediately following treatment, and typically took approximately 20 minutes. Storage time (from tissue arrival until treatment) and measurement time (which could cause some evaporation) were found to have a negligible effect on corneal thickness. Also, differences in Brillouin modulus under similar treatment conditions, but slightly different times postmortem (within the same session) were negligible. On the other hand, soaking times, and the solution used in the photosensitizer produced significant changes in thickness and Brillouin modulus. To single out this factor, we performed sham control experiments where the entire eye followed a similar soaking protocol, but only half of the eye was exposed to UV light (see Sham control experiments subsection).

### Rheometry

For shear rheometry, a standard stress-controlled rheometer was used (AR-G2; TA Instruments, New Castle, DE) with 8-mm diameter parallel plates. At approximately 100  $\mu\text{m}$  precompression, first a strain sweep (0.01%–0.5%) was performed to determine the region of linear elastic regime. Then, frequency sweeps from 0.1 to 10 Hz with 0.1% strain amplitude at 23°C were done. The data reported here refer to the shear modulus measured at approximately 0.2 Hz.

## Epi-Off Corneal Collagen Crosslinking Protocols

The corneal epithelium of the porcine eye was removed by gentle scraping with a blade (Parker #15; BD Biosciences, San Diego, CA). Riboflavin (riboflavin-5-phosphate; Sigma-Aldrich, St. Louis, MO) was diluted in dextran 8% aqueous solution to a riboflavin concentration of 0.1%. In the standard procedure, the corneas were presoaked in the riboflavin solution for 30 minutes and then exposed to a UV lamp ( $\lambda = 365$  nm, 3 mW/cm<sup>2</sup>) for 30 minutes ( $N = 6$ ). To investigate the light/soak dependence, the following combinations of photosensitizer soaking time and UV light exposure times were tested: 30 minutes presoaking with 5 minutes of UV light exposure ( $N = 2$ ); 5 minutes presoaking with 30 minutes UV exposure ( $N = 3$ ); fixed presoaking time of 30 minutes, and 0 ( $N = 3$ ), 5 ( $N = 2$ ), and 15 minutes ( $N = 2$ ) of UV light exposure.

## Transepithelial Corneal Collagen Crosslinking Protocol

For the epi-on procedure, the riboflavin solution (at 0.1%) was based on PBS without dextran. The solution contained an epithelium-loosening agent, 0.02% benzalkonium chloride (BAC), and optimized osmolarity (NaCl 0.44%) according to the protocol by Raiskup et al.<sup>33</sup> Corneas were presoaked in the solution for 30 minutes and then exposed to the UV light ( $\lambda = 365$  nm, 3 mW/cm<sup>2</sup>) for 30 minutes.

## Sham Control Experiments

Sham controls were performed for an epi-off protocol (30-minute soaking with riboflavin/dextran solution) and an epi-on protocol (30-minute soaking with riboflavin/PBS-BAC-NaCl solution). In these sets of eyes ( $N = 2$  for each condition), after soaking, one-half of the eye was blocked and the other half irradiated with UV light for 30 minutes. These controls guarantee identical timing, protocols, and solution-dependent hydration states for a given condition, with the UV-irradiation being the only distinctive parameter.

## RESULTS

### In Situ Mechanical Characterization of Corneas after Standard CXL

Figure 1 shows the measurement results by Brillouin microscopy for the standard CXL procedure. Porcine corneas crosslinked following epithelial debridement, 30-minute presoak, and using 30 minutes of UV light exposure are compared to the untreated controls. Figures 1a and 1b show representative cross-sectional images (x-z plane) of the central portions of the cornea. The color-coding of Brillouin image reveals the depth-dependent variation of Brillouin shift (and elastic modulus), and the remarkable stiffening induced by crosslinking. For better visualization of the depth-dependence of corneal elasticity, the depth profiles of Brillouin shift were computed from the cross-sectional images by averaging over the transverse axis. Figure 1c shows the representative depth profiles for treated and untreated corneas. For each sample group, the depth profiles were highly consistent from sample to sample. The profiles clearly show the distinctly different modulus values between crosslinked and untreated corneas. The depth-averaged modulus in each of the anterior, mid, and posterior regions was calculated. A total of 6 crosslinked corneas and 3 untreated controls was used for this analysis. The increase in the mean modulus is remarkable in the anterior third of the cornea (unpaired *t*-test,  $P < 0.005$ ), and it is less substantial but still highly statistically significant in the mid-stromal region (unpaired *t*-test,  $P < 0.005$ ). No changes were detected in the posterior stromal region. These features are consistent with previous literature and CXL modeling.<sup>34,35</sup>

## Effect of Presoaking Time and UV Light Exposure Time

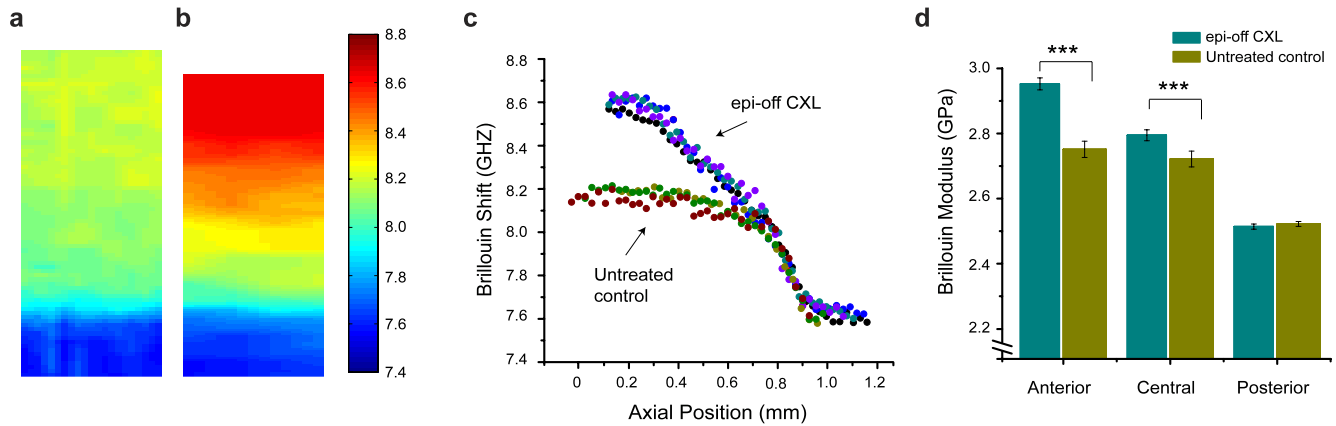
The dependence of the modulus change on two main parameters of CXL procedure, the photosensitizer presoaking time and the total optical energy, was evaluated. Figure 2 depicts the comparison of Brillouin modulus in the anterior, middle, and posterior region in four different conditions: untreated, 30-minute presoaking with 5-minute UV light exposure, 5-minute presoaking with 30-minute UV light, and 30-minute presoaking with 30-minute UV light exposure (standard Dresden protocol). From the Brillouin depth profiles and the average refractive index of 1.376 for corneal tissues, we measured the corneal thickness to be  $0.98 \pm 0.035$  mm for untreated controls,  $0.88 \pm 0.05$  mm for 30-minute presoak/5-minute light,  $0.87 \pm 0.03$  mm for 5-minute presoak/30-minute light, and  $0.84 \pm 0.03$  mm for crosslinked corneas. All treatments induced statistically significant stiffening compared to the control in the anterior and mid stroma regions (unpaired *t*-test,  $P < 0.01$ ), whereas no significant changes occurred in the posterior region. However, significant differences (unpaired *t*-test,  $P < 0.01$ ) were measured between the soaking times of 5 and 30 minutes, and between two illumination times of 5 and 30 minutes. At a soaking time of 5 minutes, the stiffness increase was reduced by 35 to 40% compared to standard Dresden protocol (i.e., CSI = 60–65). On the other hand, reducing light illumination to 5 minutes reduced mechanical efficacy by 65% to 70% (i.e., CSI = 35).

Figure 3 studies the dependence of CXL mechanical efficacy on the light exposure time by showing the corneal modulus of the anterior, central, and posterior regions for UV light exposure time varying from 0 to 30 minutes with a fixed 30-minute presoaking time. As shown in Figure 3a, the posterior region on the cornea was not stiffened at any light exposure. In the mid stromal region, only the full 30 minutes of light exposure produced a significant increase in modulus (unpaired *t*-test,  $P < 0.01$ ), and in the anterior portion of the cornea a clear dose-dependence of corneal stiffening to light exposure was observed. Figure 3b shows a highly significant linear dependence of the relative increase in anterior modulus on the light exposure time ( $R^2 > 0.98$ ). The presoaking alone (without light) induced significant stiffening (unpaired *t*-test,  $P < 0.01$ ), as a result of corneal dehydration induced by the dextran-based solution. The mechanical effect of dehydration is discussed further in the next sections.

### Corneal Collagen Crosslinking without Epithelial Debridement

Figure 4 shows the results on the mechanical efficacy of a transepithelial (“epi-on”) modality<sup>36</sup> evaluated by Brillouin microscopy. The Brillouin cross-sectional images and depth-profiles of a control (epi-on, 30 minutes presoak, no light) versus a CXL treated cornea (epi-on, 30 minutes presoak, 30 minutes light) showed that the transepithelial CXL protocol was, indeed, capable of inducing corneal stiffening (unpaired *t*-test,  $P < 0.01$ ). However, the stiffening effect was lower than the one produced by the standard CXL protocol and was confined mostly to the anterior portion of the cornea (Fig. 4d). From the Brillouin depth profiles, the corneal thickness was estimated to be  $1.12 \pm 0.02$  mm for controls and  $1.05 \pm 0.02$  mm for crosslinked corneas. To estimate the overall efficacy of transepithelial CXL, CSI was calculated by averaging the modulus over the entire corneal depth and comparing it to standard CXL. From the Brillouin measurement, the epi-on CXL was estimated to induce approximately 33% of the stiffening of epi-off CXL (i.e., CSI = 33). For comparison, the mechanical stiffening of the two procedures was tested with gold-standard





**FIGURE 1.** Brillouin mechanical characterization of standard epi-off CXL procedure. (a) A representative cross-sectional Brillouin image of normal porcine cornea. (b) A Brillouin image of the cornea after the standard CXL. The *horizontal* and *vertical* span is 0.05 mm (x) by 1.2 mm (z) in (a, b). (c) Brillouin depth profiles of crosslinked and untreated corneas. (d) Mean Brillouin modulus of the anterior, mid, and posterior regions for the crosslinked ( $N = 6$ ) versus untreated corneas ( $N = 3$ ).  $***P < 0.005$ .

quasi-static rheology. This measurement showed that epi-on CXL induced stiffening of approximately 39% (i.e., CSI = 39), consistent with the Brillouin-based measurement. As the experiments were performed *ex vivo* immediately after the CXL procedure, this estimation includes the mechanical effect of the notably different hydration states of the cornea in the epi-on versus epi-off procedure.

**Sham Controls**

Sham control experiments were performed to evaluate the effects of different parameters (e.g., timing, soaking, evaporation) within the CXL procedure. UV light was administered to only a half of the eye after riboflavin soaking, whereas the other half of the eye was blocked during UV illumination. Figures 5a and 5b show the results for the epi-off protocol and the epi-on protocol, respectively. The Brillouin profiles of the UV-illuminated region and unilluminated (sham) region of the eye are shown, along with the average Brillouin profile of untreated controls before soaking. As expected, the epi-off CXL

profile in Figure 5a and the epi-on CXL profile in Figure 5b are consistent with the ones in Figure 1c and Figure 4c, respectively. Importantly, the Brillouin moduli for the sham regions in Figure 5a and Figure 5b are equivalent to the results obtained with the controls used in Figures 1 to 3 and Figure 4, respectively. These control data were obtained with different

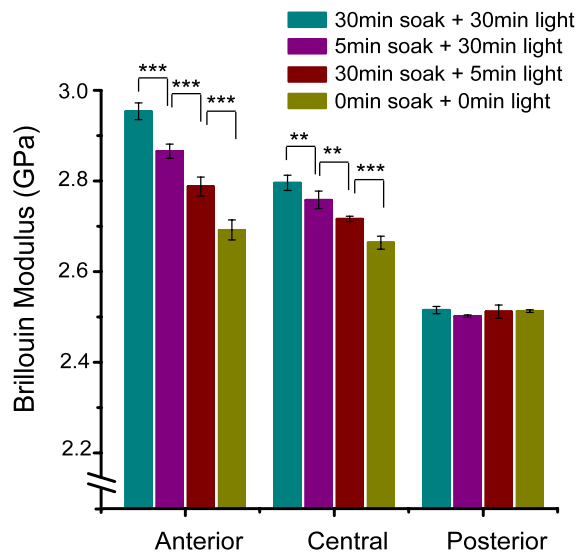


**FIGURE 2.** The effects of the varying soaking time and light exposure time on the mean Brillouin modulus of the anterior, mid, and posterior cornea.  $**P < 0.01$ ,  $***P < 0.005$ .

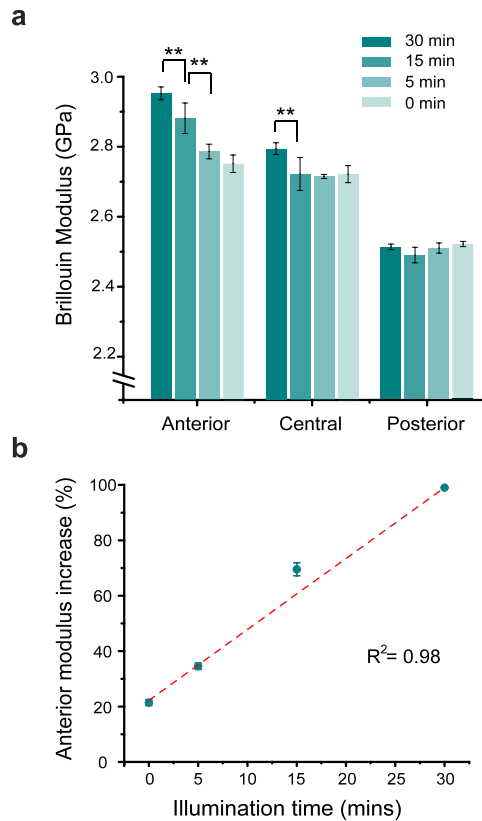


**FIGURE 3.** Mechanical outcome dependence on the light exposure time. (a) Mean Brillouin modulus of the anterior, mid, and posterior regions in the corneas treated with a presoaking time of 30 minutes, and various UV exposure times of 0, 5, 15, and 30 minutes, respectively.  $**P < 0.01$ . (b) The increase of mean Brillouin modulus in the anterior region as a function of exposure time. *Circles:* data. *Error bars:* standard deviations. *Line:* linear curve fit.

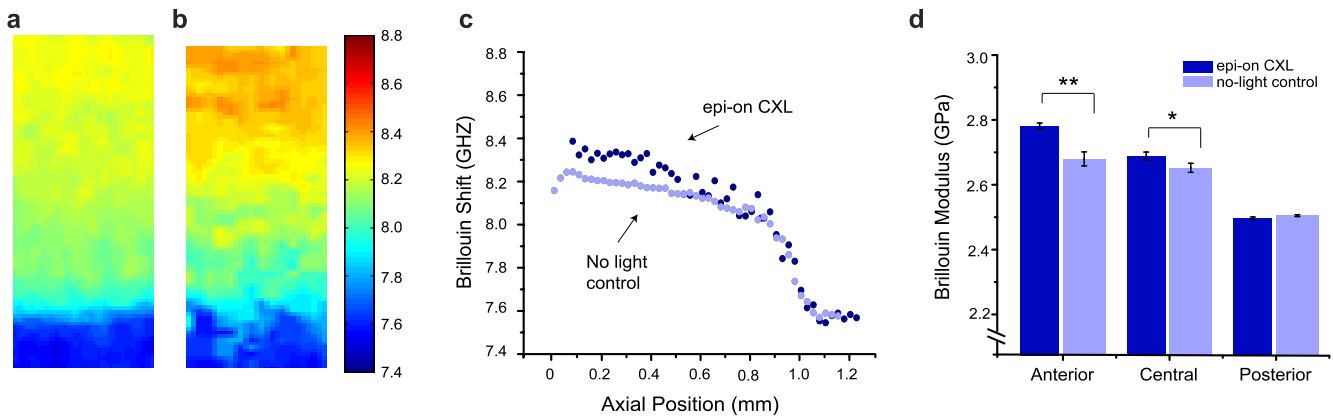


**FIGURE 4.** Brillouin mechanical characterization of transepithelial “epi-on” CXL. (a) A representative cross-sectional Brillouin image of normal porcine cornea. (b) A Brillouin image of the cornea after epi-on CXL. The horizontal and vertical span is 0.05 mm (x) by 1.2 mm (z) in (a, b). (c) Brillouin depth profile of epi-on CXL versus Soaked, but not illuminated control cornea. (d) Mean Brillouin modulus of the anterior, mid-, and posterior regions for epi-on crosslinked ( $N = 2$ ) versus untreated corneas ( $N = 2$ ). \* $P < 0.05$ , \*\*\* $P < 0.005$ .

storage times (up to 60 minutes) of the samples and varying waiting times (up to 30 minutes) between treatment and measurements. We concluded that within the short term of our experiments, differences in storage time or exposure to air had negligible effect on Brillouin modulus. On the other hand, the hydration and dehydration effects due to soaking solutions had significant mechanical effects, as noted previously (Fig. 3). These effects are described in more detail below.

**Hydration Effects on Brillouin Modulus and Shear Modulus**

As expected, the epi-off dextran-based soaking caused the cornea to dehydrate (thickness =  $0.90 \pm 0.03$  mm) while the epi-on saline-based soaking induced corneal swelling (thickness =  $1.12 \pm 0.02$  mm). Figure 5 indicates that corneal dehydration is associated with an increased Brillouin modulus, whereas corneal hydration decreases Brillouin modulus. The dehydration caused by the application of dextran solution alone caused significant corneal stiffening with a CSI of approximately 20. To validate this observation, gold-standard bulk rheology was used to compare shear modulus in samples

soaked in dextran-based and saline-based solutions. As shown in Figure 6, corneas soaked with dextran-based epi-off solution had significantly higher shear moduli than corneas soaked with saline-based epi-on solution. This result is consistent with our Brillouin measurements.

**DISCUSSION**

Most CXL procedures tested around the world follow the original protocol described by Wollensak et al., which involves epithelial debridement, 30-minute soaking in riboflavin-dextran solution and a 30-minute application of UV light.<sup>3</sup> However, the significant thinning induced by the riboflavin-dextran solution during the procedure and the fear of endothelial cell damage make standard CXL only applicable to thicker corneas (>350  $\mu$ m). Moreover, the requirement of epithelial debridement to enable riboflavin diffusion into the corneal stroma results in significant eye pain in the first few days of postoperative recovery and increased risk of infections.<sup>37</sup> For these reasons, a significant effort has been undertaken to develop alternative procedures that result in reduced thinning, phototoxicity, and recovery time, while

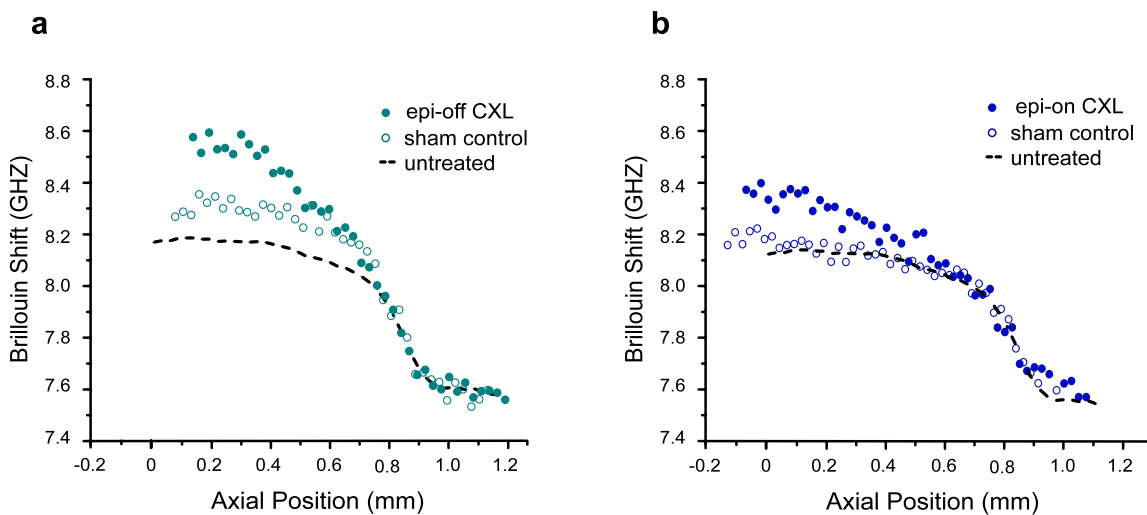


**FIGURE 5.** Mechanical effect of the corneal hydration state. (a) Brillouin depth profile of epi-off CXL versus sham control (nonilluminated area of the same cornea). Dashed line indicates the average profile of untreated controls. (b) Brillouin depth profile of epi-on CXL versus sham control. Dashed line indicates the average profile of untreated controls.

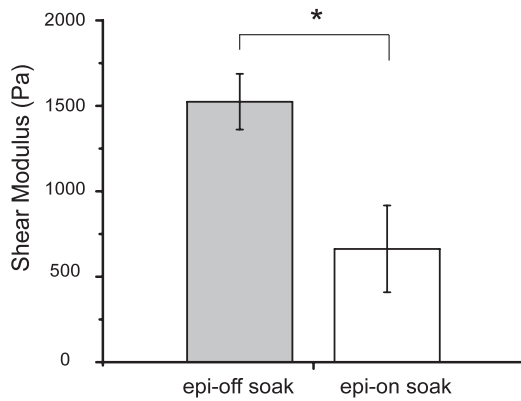


**FIGURE 6.** Shear modulus at 0.2 Hz of central corneal button (4 mm diameter). Buttons were resected and immersed in epi-off (dextran-based) solution ( $N = 6$ ) versus epi-on (saline-based) soaking ( $N = 6$ ) for 30 minutes before measurement. Error bars: SEM. \* $P < 0.05$ .

obtaining similar mechanical outcomes. In this context, transepithelial CXL,<sup>7,10</sup> custom epithelial debridement,<sup>9</sup> and hypo-osmolar photosensitizer solution<sup>8</sup> have been developed. However, the lack of a technology to monitor the mechanical outcome of various protocols has compromised the development of optimized CXL protocols.

In our study, novel Brillouin microscopy was used to perform high-resolution noncontact and noninvasive mechanical characterization of corneas from intact eyes before and after CXL *ex vivo* in several settings relevant for application in the clinic. Brillouin microscopy enabled us to determine quantitatively the mechanical efficacy of various CXL protocols. We introduced a universal metric to quantify the stiffening due to a certain CXL procedure relative to standard Dresden protocol. The Table summarizes the CSI measured using Brillouin microscopy.

From the Brillouin elasticity images, it was found that corneal stiffening occurs in a depth-dependent manner with most of the mechanical changes concentrated in the anterior portion of the corneal stroma. This result can be understood by considering the gradient of riboflavin diffusion along depth and the diminished light energy delivered to deep layers of the cornea due to absorption of the riboflavin in the anterior cornea.<sup>38-40</sup> Similar depth-dependence of corneal stiffening has been observed previously in a destructive mechanical test by Kohlhaas et al.,<sup>34</sup> who physically sectioned corneas at three different depths and observed a significant increase in the modulus of the anterior portion of the stroma, but no increase in the mid stromal region. In our study Brillouin microscopy revealed a noticeable increase of the corneal modulus also in the central portion of the stroma. This result is consistent with the recent experimental and modeling studies that predicted a larger increase in the anterior stroma than Kohlhaas et al., and a significant increase of modulus also in the mid stroma section.<sup>35</sup> It would be interesting to test if these results can be reproduced with other advanced mechanical measurement techniques.<sup>41,42</sup>

The results of our study provide an insight into how the presoaking time and light dose affect the corneal mechanical outcome. A reduction of the presoaking time from 30 to 5 minutes reduced the effectiveness of crosslinking protocols by approximately 30% in terms of the increase of the corneal stiffness. The light exposure time was found to be a much more significant factor. A clear linear dependence was measured between the relative increase in anterior corneal modulus and UV light exposure time. This result is consistent

**TABLE.** Mechanical Efficacy of Various CXL Procedure Quantified by the Defined Corneal Stiffening Index

| CXL Procedure                    | Corneal Stiffening Index |
|----------------------------------|--------------------------|
| Untreated                        | 0                        |
| Epi-on 30 min BAC + 30 min light | 33                       |
| Epi-off 30 min Rf + 5 min light  | 37                       |
| Epi-off 30 min Rf + 15 min light | 58                       |
| Epi-off 5 min Rf + 30 min light  | 65                       |
| Epi-off 30 min Rf + 30 min light | 100                      |

Rf, riboflavin-dextran; BAC, benzalkonium chloride.

with recent studies of riboflavin UV-crosslinking, which showed a linear dependence of the relative stiffness increase to total amount of UV energy absorbed.<sup>35</sup> In the central portion of the cornea, only the full 30 minutes of light illumination introduced a statistically significant increase in corneal modulus.

In the study of the transepithelial CXL protocol, a clear depth-dependent stiffening was observed within the cornea with a statistically significant increase of corneal modulus in anterior and central regions of the stroma. The epi-on procedure was found to yield a CSI of 33, that is approximately one third of the mechanical efficacy of the standard CXL protocol. This estimation was validated with bulk rheology, which measured a CSI of 39, a reasonable agreement with the Brillouin measurement. The significant reduction in the mechanical efficacy of the epi-on procedure probably is the main factor responsible for the inferior clinical outcome demonstrated by recent clinical studies.<sup>43</sup>

A prior study that attempted to quantify the mechanical efficacy of transepithelial CXL found epi-on CXL to be approximately one fifth as efficient as the standard CXL (i.e., CSI = 20).<sup>7</sup> The increased mechanical efficacy of this study is attributed to the improved protocol used for photosensitizer diffusion, developed by Raiskup et al.<sup>33</sup> It should be noted that the epi-on CXL protocol may be less effective for the porcine corneas than human corneas, because porcine corneas have thicker epithelium than human corneas.<sup>36</sup>

Finally, the hydration state of the cornea was found to be relevant when assessing the mechanical efficacy as it contributes significantly to the mechanical properties of the cornea. This effect is important particularly for CXL procedures, because the mechanical change due to corneal hydration is, for the most part, a transient effect and patients are expected to restore their normal hydration state in the long term.<sup>44,45</sup> In this investigation, dehydration was measured to increase the corneal modulus whereas hydration decreased corneal modulus, which is in agreement with previous studies on corneas and other soft biological tissues.<sup>46,47</sup> This effect was measured with Brillouin microscopy and confirmed with bulk rheology (Fig. 6). The effect of hydration also is relevant to the long-term mechanical efficacy of the epi-on procedure, because the soaking solution of epi-on CXL is based on PBS and, thus, tends to hydrate the cornea, whereas the epi-off procedure uses dextran, which dehydrates the cornea and results in a CSI as high as 20.

In conclusion, our study has demonstrated that Brillouin microscopy is an accurate and useful tool to monitor and determine the mechanical outcome of CXL in intact eyes at high spatial resolution. The dependence of the mechanical outcome on several operational parameters with and without epithelial debridement has been characterized and quantified in terms of a universal metric, CSI. Given the importance of the mechanical effect of hydration state and the transient nature of

corneal hydration/dehydration due to CXL procedure, our study suggested that judging the long-term mechanical efficacy of CXL may require in vivo estimations. As Brillouin microscopy has been demonstrated recently in vivo,<sup>25</sup> this technology may prove useful not only in the preclinical setting to develop new crosslinking agents and optimize CXL protocols, but also in the clinic as a monitoring tool to evaluate rapidly and follow longitudinally the mechanical outcome of the treatment.

### Acknowledgments

The authors thank Irene E. Kochevar, Cynthia J. Roberts, Tom Gisel, and Eri Verter for helpful discussions.

### References

- Dupps WJ. Biomechanical modeling of corneal ectasia. *J Refract Surg.* 2005;21:186-190.
- Wollensak G. Crosslinking treatment of progressive keratoconus: new hope. *Curr Opin Ophthalmol.* 2006;17:356-360.
- Wollensak G, Spoerl E, Seiler T. Riboflavin/ultraviolet-A-induced collagen crosslinking for the treatment of keratoconus. *Amer J Ophthalmol.* 2003;135:620-627.
- Caporossi A, Baiocchi S, Mazzotta C, Traversi C, Caporossi T. Parasurgical therapy for keratoconus by riboflavin-ultraviolet type A rays induced cross-linking of corneal collagen: preliminary refractive results in an Italian study. *J Cataract Refract Surg.* 2006;32:837-845.
- Raiskup-Wolf F, Hoyer A, Spoerl E, Pillunat LE. Collagen crosslinking with riboflavin and ultraviolet-A light in keratoconus: long-term results. *J Cataract Refract Surg.* 2008;34:796-801.
- Wittig-Silva C, Whiting M, Lamoreaux E, Lindsay RG, Sullivan LJ, Snibson GR. Randomized controlled trial of corneal collagen cross-linking in progressive keratoconus: preliminary results. *J Refract Surg.* 2008;24:S720-S725.
- Wollensak G, Iomdina E. Biomechanical and histological changes after corneal crosslinking with and without epithelial debridement. *J Cataract Refract Surg.* 2009;35:540-546.
- Hafezi F, Mrochen M, Iseli HP, Seiler T. Collagen crosslinking with ultraviolet-A and hypoosmolar riboflavin solution in thin corneas. *J Cataract Refract Surg.* 2009;35:621-624.
- Kymionis GD, Diakonis VF, Coskunseven E, Jankov M, Yoo SH, Pallikaris IG. Customized pachymetric guided epithelial debridement for corneal collagen cross linking. *BMC Ophthalmol.* 2009;9:10.
- Yuen L, Chan C, Wachler BSB. Effect of epithelial debridement in corneal collagen crosslinking therapy in porcine and human eyes. *J Cataract Refract Surg.* 2008;34:1815-1816.
- Discher D, Dong C, Fredberg JJ, et al. Biomechanics: cell research and applications for the next decade. *Ann Biomed Eng.* 2009;37:847-859.
- Luce DA. Determining in vivo biomechanical properties of the cornea with an ocular response analyzer. *J Cataract Refract Surg.* 2005;31:156-162.
- Shah S, Laiquzzaman M, Bhojwani R, Mantry S, Cunliffe I. Assessment of the biomechanical properties of the cornea with the ocular response analyzer in normal and keratoconic eyes. *Invest Ophthalmol Vis Sci.* 2007;48:3026-3031.
- Spoerl E, Terai N, Scholz F, Raiskup F, Pillunat LE. Detection of biomechanical changes after corneal cross-linking using ocular response analyzer software. *J Refract Surg.* 2011;27:452-457.
- Fontes BM, Ambrosio R Jr, Velarde GC, Nose W. Ocular response analyzer measurements in keratoconus with normal central corneal thickness compared with matched normal control eyes. *J Refract Surg.* 2011;27:209-215.
- Fontes BM, Ambrosio R Jr, Jardim D, Velarde GC, Nose W. Corneal biomechanical metrics and anterior segment parameters in mild keratoconus. *Ophthalmology.* 2011;117:673-679.
- Dorransoro C, Pascual D, Perez-Merino P, Kling S, Marcos S. Dynamic OCT measurement of corneal deformation by an air puff in normal and cross-linked corneas. *Biomed Opt Exp.* 2012;3:473-487.
- Wang HC, Prendiville PL, McDonnell PJ, Chang WV. An ultrasonic technique for the measurement of the elastic moduli of human cornea. *J Biomech.* 1996;29:1633-1636.
- He X, Liu JA. Quantitative ultrasonic spectroscopy method for noninvasive determination of corneal biomechanical properties. *Invest Ophthalmol Vis Sci.* 2009;50:5148-5154.
- Ambrosio R Jr, Caldas D, Ramos I, Santos R, Belin M. *Corneal Biomechanical Assessment Using Dynamic Ultra High-Speed Scheimpflug Technology Non-contact Tonometry (UHS-ST NCT): Preliminary Results.* Presented at the American Society of Cataract and Refractive Surgery-American Society of Ophthalmic Administrators (ASCRS-ASOA) Symposium and Congress. San Diego, CA, March 25-29, 2011.
- Ford MR, Dupps WJ Jr, Rollins AM, Roy AS, Hu Z. Method for optical coherence elastography of the cornea. *J Biomed Opt.* 2011;16:016005.
- Grabner G, Eilmsteiner R, Steindl C, Ruckhofer J, Mattioli R, Husinsky W. Dynamic corneal imaging. *J Cataract Refract Surg.* 2005;31:163-174.
- Scarcelli G, Yun SH. Confocal Brillouin microscopy for three-dimensional mechanical imaging. *Nat Photonics.* 2008;2:39-43.
- Scarcelli G, Pineda R, Yun S. Brillouin optical microscopy for corneal biomechanics. *Invest Ophthalmol Vis Sci.* 2012;53:185-190.
- Scarcelli G, Yun SH. In vivo Brillouin optical microscopy of the human eye. *Opt Express.* 2012;20:9197-9202.
- Scarcelli G, Kim P, Yun SH. Cross-axis cascading of spectral dispersion. *Opt Lett.* 2008;33:2979-2981.
- Scarcelli G, Yun SH. Multistage VIPA etalons for high-extinction parallel Brillouin spectroscopy. *Opt Express.* 2011;19:10913-10922.
- Randall J, Vaughan JM. The measurement and interpretation of Brillouin scattering in the lens of the eye. *Proc R Soc Lond B Biol Sci.* 1982;214:449-470.
- Kikkawa Y, Hirayama K. Uneven swelling of corneal stroma. *Invest Ophthalmol.* 1970;9:735-741.
- Wilson G, O'Leary DJ, Vaughan W. Differential swelling in compartments of the corneal stroma. *Invest Ophthalmol Vis Sci.* 1984;25:1105-1108.
- Ortiz S, Siedlecki D, Grulkowski I, et al. Optical distortion correction in optical coherence tomography for quantitative ocular anterior segment by three-dimensional imaging. *Opt Express.* 2010;18:2782-2796.
- Scarcelli G, Kim P, Yun SH. In vivo measurement of age-related stiffening in the crystalline lens by Brillouin optical microscopy. *Biophys J.* 2011;101:1539-1545.
- Raiskup F, Pinelli R, Spoerl E. Riboflavin osmolar modification for transepithelial corneal cross-linking. *Curr Eye Res.* 2012;37:234-238.
- Kohlhaas M, Spoerl E, Schilde T, Unger G, Wittig C, Pillunat LE. Biomechanical evidence of the distribution of cross-links in corneas treated with riboflavin and ultraviolet A light. *J Cataract Refract Surg.* 2006;32:279-283.
- Schumacher S, Mrochen M, Wernli J, Bueeler M, Seiler T. Optimization model for uv-riboflavin corneal cross-linking. *Invest Ophthalmol Vis Sci.* 2012;53:762-769.
- Kissner A, Spoerl E, Jung R, Spekl K, Pillunat LE, Raiskup F. Pharmacological modification of the epithelial permeability by

- benzalkonium chloride in UVA/riboflavin corneal collagen cross-linking. *Curr Eye Res.* 2010;35:715-721.
37. Suri K, Hammersmith KM, Nagra PK. Corneal collagen cross-linking: ectasia and beyond. *Curr Opin Ophthalmol.* 2012;23:280-287.
  38. Bueno JM, Gualda EJ, Giakoumaki A, Pérez-Merino P, Marcos S, Artal P. Multiphoton microscopy of ex vivo corneas after collagen cross-linking. *Invest Ophthalmol Vis Sci.* 2011;52:5325-5331.
  39. Sondergaard AP, Hjortdal J, Breitenbach T, Ivarsen A. Corneal distribution of riboflavin prior to collagen cross-linking. *Curr Eye Res.* 2010;35:116-121.
  40. Spoerl E, Raiskup-Wolf F, Pillunat LE. Biophysical principles of collagen cross-linking. *Klin Monbl Augenheilkd.* 2008;225:131-137.
  41. Kling S, Ginis H, Marcos S. Corneal biomechanical properties from two-dimensional corneal flap extensimetry: application to UV-riboflavin cross-linking. *Invest Ophthalmol Vis Sci.* 2012;53:5010-5015.
  42. Kling S, Remon L, Perez-Escudero A, Merayo-Llodes J, Marcos S. Corneal biomechanical changes after collagen cross-linking from porcine eye inflation experiments. *Invest Ophthalmol Vis Sci.* 2010;51:3961-3968.
  43. Koppen C, Wouters K, Mathysen D, Rozema J, Tassignon MJ. Refractive and topographic results of benzalkonium chloride-assisted transepithelial crosslinking. *J Cataract Refract Surg.* 2012;38:1000-1005.
  44. Holopainen JM, Krootila K. Transient corneal thinning in eyes undergoing corneal cross-linking. *Amer J Ophthalmol.* 2011;152:533-536.
  45. Kymionis GD, Kounis GA, Portaliou DM, et al. Intraoperative pachymetric measurements during corneal collagen cross-linking with riboflavin and ultraviolet A irradiation. *Ophthalmology.* 2009;116:2336-2339.
  46. Jayasuriya AC, Scheinbeim JI, Lubkin V, Bennett G, Kramer P. Piezoelectric and mechanical properties in bovine cornea. *J Biomed Mater Res A.* 2003;66:260-265.
  47. Nicolle S, Paliarne JF. Dehydration effect on the mechanical behaviour of biological soft tissues: observations on kidney tissues. *J Mech Behav Biomed Mat.* 2010;3:630-635.